

Studies of New Antiferroelectric Liquid Crystal Based on Quantum-Chemical Model

W. TOMCZYK^{a,*}, M. MARZEC^a, E. JUSZYŃSKA^b, R. DĄBROWSKI^c, D. ZIOBRO^c, S. WRÓBEL^a
AND M. MASSALSKA-ARODŹ^b

^aInstitute of Physics, Jagiellonian University, W.S. Reymonta 4, 30-059 Kraków, Poland

^bInstitute of Nuclear Physics, Polish Academy of Sciences, E. Radzikowskiego 152, 31-342 Kraków, Poland

^cMilitary University of Technology, S. Kaliskiego 2, 00-908 Warszawa, Poland

Physical properties of new thermotropic antiferroelectric liquid crystal have been studied. Experiments were done by use of complementary methods such as differential scanning calorimetry, polarizing optical microscopy and X-ray powder diffractometry. Acquired data from X-ray powder diffractometry was examined under application of quantum chemical approach. It has been found that compound studied exhibits stable enantiotropic antiferroelectric SmC_A^{*} phase in the wide temperature range while ferroelectric phase SmC^{*} is very narrow.

DOI: 10.12693/APhysPolA.124.949

PACS: 77.84.Nh, 64.70.M-

1. Introduction

For more than 125 years [1] liquid crystals are of a great interest due to their unusual properties and possible applications. Synthesis of new liquid crystal compounds and results of experiments are the main key points on the way to broaden the knowledge about undeniably remarkable liquid crystal state. In recent years, particular attention was focused on ferroelectric (FLC) and antiferroelectric (AFLC) liquid crystals [2] which are expected to significantly improve the image quality of liquid crystal displays (LCD). As for now it has been proved that such improvement can be acquired with a use of mixtures. Thus, it is essential to find a compound that could be a basis for such mixture, e.g. having properties satisfying all technical assumptions.

Antiferroelectric SmC_A^{*} liquid crystalline phase [3] were discovered soon after the ferroelectric SmC^{*} [4]. Both exhibit similar properties: tilted molecules due to chiral atoms and existence of spontaneous polarization, but the difference is in the director of the neighboring layers, e.g. the director is tilted in opposite direction in alternate layers in the antiferroelectric phase. Antiferroelectric phase occurs always, if it is, at the temperature below the ferroelectric one [5, 6].

The aim of this paper is to study physical and chemical properties of new liquid crystalline compound exhibiting both ferroelectric SmC^{*} and antiferroelectric SmC_A^{*} phases. The main subject of this work is the comparison of the proposed molecules' model with the experimental results.

2. Experimental

In this paper the new thermotropic liquid crystal compound [4-[4-[4-(2,2,3,3,4,4,5,5,6,6,7,7,7-tridecafluoro-

heptanoyloxy)butoxy]phenyl]phenyl]4-[(1R)-1 methyl-hepto-xy]benzoate, abbreviated 6F4BBiOC8 [7] has been studied. The molecular structure is presented in Fig. 1. As it is seen it has a rod-like structure, which was onward verified by density functional theory (DFT) methods, like it is shown in Fig. 2. Due to the existence of chiral centre in the molecule, existence of the ferroelectric SmC^{*} phase or/and antiferroelectric SmC_A^{*} one was forecasted. Strongly fluorized group -C₆F₁₃ in opposition to alkyl chain -C₆H₁₃ induces nonzero dipole moment, which results in asymmetric charge distribution. Using Mercury 3.1 programme the length and width of the molecule was calculated. The length of 6F4BBiOC8 was estimated to be around 37.76 Å and width *ca.* 4.30 Å.

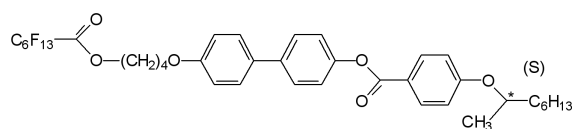


Fig. 1. Molecular structure of the substance studied — 6F4BBiOC8.

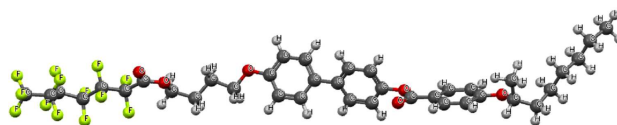


Fig. 2. Optimized geometry for 6F4BBiOC8.

DI MOND 8000 Perkin Elmer calorimeter was used with aluminum crucibles of 30 μl to registered DSC curves and find transition temperatures. Sample weight was 5.60 g. The DSC data were collected for heating/cooling rates ranges from 5 to 40 °C/min in the sequence of every 5 °C/min. Pyris Software was used to calculate the transition temperature and enthalpy changes connected with them.

*corresponding author; e-mail: wojciech.tomczyk@uj.edu.pl

Texture observation was done using NIKON Eclipse polarizing microscope with LINK M hot stage. The ITO electrooptic cell of $5\ \mu\text{m}$ thickness was used (AWAT Company, homogeneous ordering).

X-ray powder diffractometry was performed using X'PERT PRO PANalytical diffractometer with temperature regulated crucible. Experiment was done at heating and cooling in the temperature range between $25\ ^\circ\text{C}$ and $125\ ^\circ\text{C}$ with the sequence of every $5\ ^\circ\text{C}$ with 10 min temperature relaxation. X'Pert High Score Programme was used to find diffraction maxima. The resolve and assign of the unit cell from experimental data was done with the application of X-Cell algorithm [8].

Quantum chemical computations to optimize geometry of the molecule were made basing on DFT [9, 10] implemented in the Dmol³ programme from Accelrys's Materials Studio 5.5 environment. For the description of correlation-exchange interactions the gradient functional was used (general gradient approximation (GG)) [11] in Perdew–Burke–Ernzerhof (PBE) parameterization [12]. Calculations were made using numeric functional base, centralized on atoms with double numerical with polarization (DNP) precision. Convergence criterion SCF had been established on and energetic convergence criterion for searching the optimal geometry was set at 10^{-6} Ha. DFT semicore pseudopotential (DSPP) was used to describe the behaviour of the core electrons.

Theoretical approach based on quantum-chemical models gives us a broader view on interactions that occur in molecule's local environment. It is a way to visualize how molecular mechanisms influences the behaviour of the molecule, which leads to deeper conclusions.

3. Results and discussion

Based on DSC results the essential information about phase transitions which occurs in 6F4BBiOC8 has been gathered. As it is seen in Fig. 3, the heating/cooling rates do not influence so much on the transition temperatures as well as on number of anomalies appearing on the DSC curves. Data acquired from DSC calorimetry are gath-

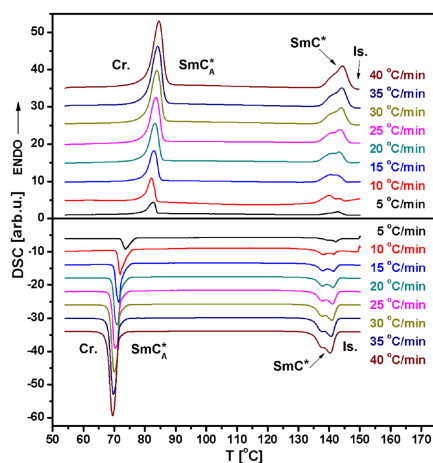


Fig. 3. DSC curves registered at heating and cooling for different rates.

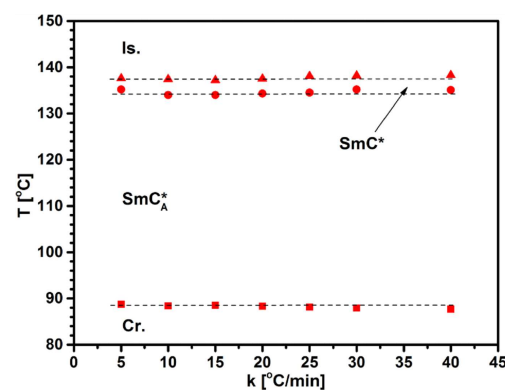


Fig. 4. Transition temperatures versus heating rate k .

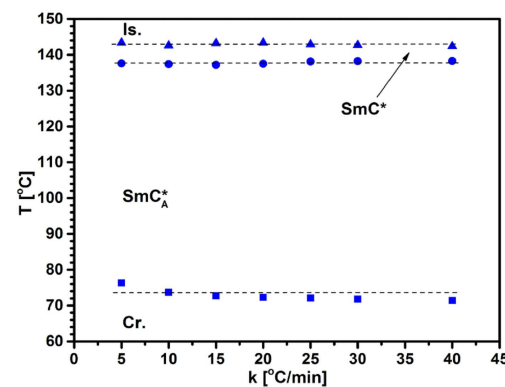


Fig. 5. Transition temperatures versus cooling rate k .

ered in Table I. Polarizing optical microscopy (POM), as a complementary method to DSC, leads to the identification of the liquid crystalline phases as SmC_A^* and SmC^* . The temperatures of the transitions versus heating and cooling rate are summarized in Fig. 4 and Fig. 5, respectively. The straight line is linear fitting to the transition temperature versus rate. Based on the fitting results, the phase sequences were obtained at so-called zero heating/cooling and they are placed at the bottom of Table I.

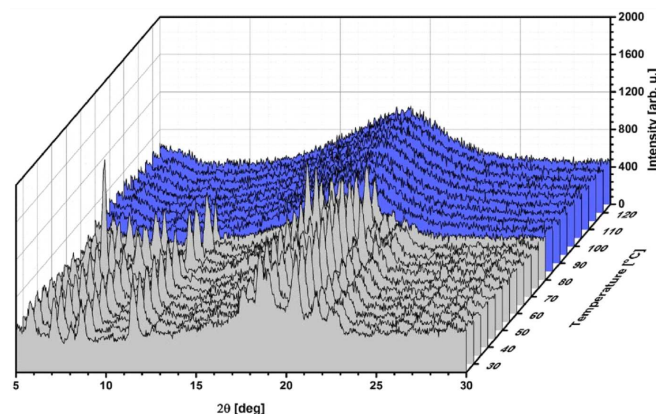


Fig. 6. 3D diffractograms acquired at heating.

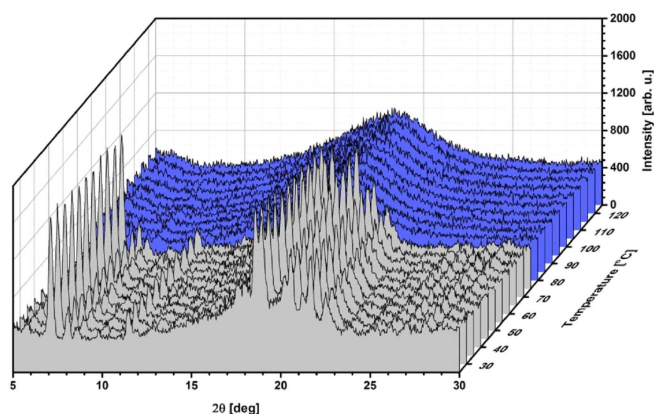


Fig. 7. 3D diffractograms acquired at cooling.

Diffractograms, which are shown in Figs. 6 and 7 demonstrate the enantiotropic character of the phases appearing in the phase sequence of the compound studied. Temperatures of the phase transitions obtained by X-ray method are consistent with the DSC and POM results within the measurement error. In the temperature range from 25°C to around 80°C, 6F4BBiOC8 exhibits an ordered structure — crystal phase while over 80°C antiferroelectric SmC_A^* phase appears. Due to its liquid-like properties there were not observed any diffraction maxima over 5°, as it is presented in Figs. 6 and 7. The wide-ranging maximum visible from 15° to 25° is connected with stochastic movements of molecules.

TABLE I

Phase transition temperatures, enthalpy and entropy changes for 6F4BBiOC8 at different cooling and heating rates k . The phase sequences at so-called zero heating/cooling rate are placed at the bottom of table.

Heating				Cooling			
k [°C/min]	T_{ONSET} [°C]	ΔH [J/g]	ΔS [J/(mol K)]	k [°C/min]	T_{ONSET} [°C]	ΔH [J/g]	ΔS [J/(mol K)]
5	79.9	19.3	45.52	5	143.4	−8.1	−16.37
	135.2	5.3	13.01		137.6	−6.3	−15.15
	137.6	8.6	17.30		76.3	−17.6	−42.68
10	79.6	20.2	47.86	10	142.6	−7.8	−16.04
	134.0	5.7	13.74		137.4	−6.1	−14.87
	136.0	9.1	18.39		73.7	−18.1	−44.03
15	80.0	20.4	48.01	15	143.2	−8.3	−16.89
	134.0	5.5	13.68		137.2	−6.5	−15.56
	136.0	9.0	18.37		72.7	−18.3	−44.68
20	80.1	19.8	46.84	20	143.4	−8.5	−17.37
	134.3	5.4	13.72		137.5	−6.7	−15.87
	136.2	9.0	18.25		72.3	−18.0	−44.16
25	80.2	20.0	47.09	25	142.9	−8.4	−17.14
	134.2	5.3	13.48		138.2	−6.6	−15.72
	136.6	8.9	17.99		72.1	−17.8	−43.67
30	80.4	19.6	46.21	30	142.7	−8.5	−17.15
	135.2	5.3	13.52		138.2	−6.6	−15.75
	138.6	8.9	17.98		71.8	−17.9	−44.00
40	80.8	19.3	45.56	40	142.4	−8.5	−18.38
	135.1	4.9	13.03		138.1	−6.7	−16.15
	138.9	8.6	17.48		71.4	−17.4	−42.60
$\text{Cr} \xrightarrow{80.3^\circ\text{C}} \text{SmC}_A^* \xrightarrow{134.0^\circ\text{C}} \text{SmC}^* \xrightarrow{138.3^\circ\text{C}} \text{Is}$				$\text{Is} \xrightarrow{143.3^\circ\text{C}} \text{SmC}^* \xrightarrow{137.8^\circ\text{C}} \text{SmC}_A^* \xrightarrow{72.7^\circ\text{C}} \text{Cr}$			

The spacing distance between layers as a function of temperature is presented in Fig. 8, while Fig. 9 presents the distribution of this distance. In low 2θ angle regime, between 1° and 5° one can see small diffraction maximum (see Fig. 10) which describes distance between the centres of molecules in the neighbouring smectic layers, e.g. the distance between adjacent layers. The crystal structure calculated is shown in Fig. 11 while the unit cell parameters are gathered in Table II.

Experimental data are matching with computational results. Molecule's geometry calculated is in good agreement with the dimensions of unit cell as well as spacing distance calculated between the centres of mass of the molecules in the smectics layer is appropriate. Similar results for the liquid crystalline compound e.g. crystallization in the same space group was reported in [13].

TABLE II

The unit cell parameters calculated.

Monoclinic	a [Å]	b [Å]	c [Å]	α [°]	β [°]	γ [°]
6F4BBiOC8	30.63	5.15	12.73	90.00	111.58	90.00
space group: $P2$		Laue class: $2/m$		point group: $2(2 Y)$		

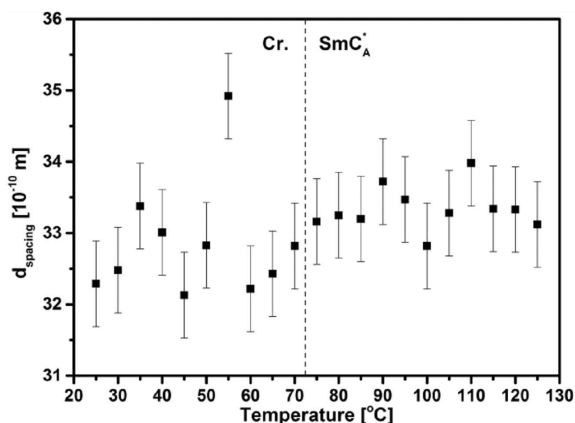


Fig. 8. Distance between layers versus temperature near phase transition at cooling.

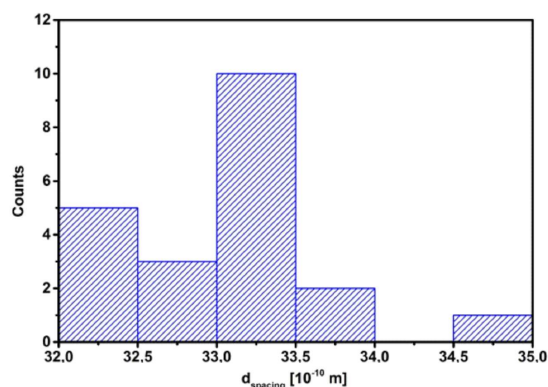


Fig. 9. Histogram showing the distribution of the layer distance.

4. Conclusion

Complementary methods were applied to study properties of antiferroelectric 6F4BBiOC8 compound. Based on differential scanning calorimetry and polarizing optical microscope methods it has been shown that substance studied exhibits a stable polymorphism, which consists of ferroelectric SmC^* and antiferroelectric SmC_A^* phases. X-ray powder diffraction gave some information about the structure and confirmed the enantiotropic character of phases appearing in the phase sequence. Based on the quantum chemical computation (optimization of the geometry of single molecule and arrangement of molecules in the space) it was possible to find out the organization of molecules of 6F4BBiOC8 in the crystal state.

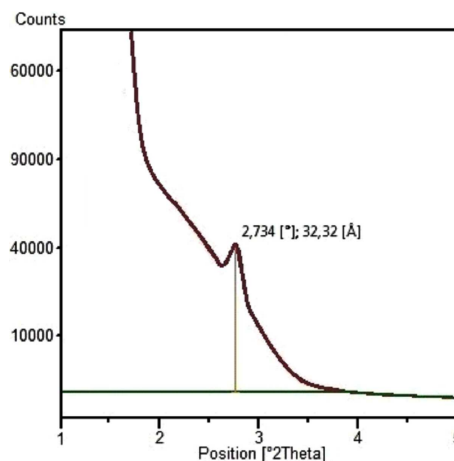


Fig. 10. Diffraction maximum registered at low angle range.

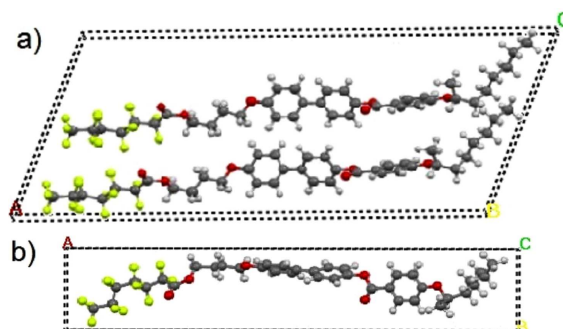


Fig. 11. The unit cell calculated along (100) (a) and (001) (b).

The wide temperature range of SmC_A^* phase is one of the important properties for compounds that might find application in LCDs, that is why the compound studied seems to be very attractive from the application point of view. Further studies are needed to check some other properties such as spontaneous polarization, tilt angle, or switching time to give an answer to question if 6F4BBiOC8 is a good material for use in LCD technology.

References

- [1] F. Reinitzer, *Monatshefte für Chemie (Wien)* **9**, 421 (1888).
- [2] S.T. Lagerwall, *Ferroelectric and Antiferroelectric Liquid Crystals*, Wiley-VCH, Germany 1999.

- [3] A.D.L. Chandani, Y. Ouchi, H. Takezoe, A. Fukuda, K. Terashima, K. Furokawa, A. Kishi, *Jpn. J. Appl. Phys.* **28**, L1261 (1989).
- [4] R.B. Meyer, L. Liebert, L. Strzelecki, P. Keller, *J. Phys. Lett. (France)* **36**, 69 (1975).
- [5] V. Hamplová, A. Bubnov, M. Kašpar, V. Novotná, Y. Lhotáková, M. Glogarová, *Liq. Cryst.* **30**, 1463 (2003).
- [6] J.M. Czerwiec, R. Dąbrowski, M. Żurowska, D. Ziobro, S. Wróbel, *Acta Phys. Pol. A* **117**, 553 (2010).
- [7] M. Marzec, W. Tomczyk, J. Czerwiec, R. Dąbrowski, S. Wróbel, D. Ziobro, *Electrooptic Studies of New Antiferroelectric Mixture*, poster, *ILCC 2012, Mainz (Germany)*.
- [8] M.A. Neumann, *J. Appl. Crystallogr.* **36**, 356 (2003).
- [9] B.K. Delley, *J. Chem. Phys.* **92**, 508 (1990).
- [10] B.K. Delley, *J. Chem. Phys.* **113**, 7756 (2000).
- [11] J.P. Perdew, K. Burke, Y. Wang, *Phys. Rev. B* **54**, 16 539 (1996).
- [12] J.P. Perdew, K. Burke, M. Ernzerhof, *Phys. Rev. Lett.* **77**, 3865 (1996).
- [13] K. Družbicki, E. Mikuli, A. Kocot, M.D. Ossowska-Chruściel, J. Chruściel, S. Zalewski, *J. Phys. Chem. A* **116**, 7809 (2012).